HDL-TM-71-35

FLUERICS 31. THE TRANSITION FROM ISOTHERMAL TO ADIABATIC CAPACITANCE IN CYLINDRICAL ENCLOSURES

by

Silas Katz

Edgar Hastie

December 1971

U.S. ARMY MATERIEL COMMAND

HARRY DIAMOND LABORATORIES

WASHINGTON, D.C. 20438

R

31

The findings in this report are not to be construed as an official Department of the Army position unless so designated by other authorized documents.

Citation of manufacturers' or trade names does not constitute an official indorsement or approval of the use thereof.

Destroy this report when it is no longer needed. Do not return it to the originator.

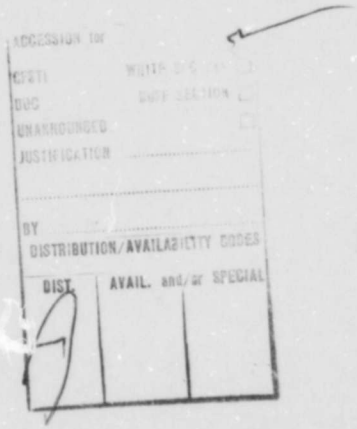

DOCUMENT CONTROL DATA - R & D

(Security classification of title, body of abstract and indexing annotation must be entered when the overall report is classified)

1. ORIGINATING ACTIVITY (Corporate author) Harry Diamond Laboratories Washington, D. C. 20438	2a. REPORT SECURITY CLASSIFICATION Unclassified 2b. GROUP

3. REPORT TITLE

Fluerics 31. The Transition from Isothermal to Adiabatic Capacitance in Cylindrical Enclosures

4. DESCRIPTIVE NOTES (Type of report and inclusive dates)

5. AUTHOR(S) (First name, middle initial, last name)

Silas Katz
Edgar Hastie

6. REPORT DATE December 1971	7a. TOTAL NO. OF PAGES 42	7b. NO. OF REFS 11
8a. CONTRACT OR GRANT NO b. PROJECT NO. DA-1T61102A33B c. AMCMS Code: 501B.11.71200 d. HDL Proj: 3FL31	9a. ORIGINATOR'S REPORT NUMBER(S) HDL-TM-71-35 9b. OTHER REPORT NO(S) (Any other numbers that may be assigned this report)	

10. DISTRIBUTION STATEMENT

Approved for public release; distribution unlimited.

11. SUPPLEMENTARY NOTES	12. SPONSORING MILITARY ACTIVITY USAMC

13. ABSTRACT

The capacitance of enclosed volumes depends on the polytropic exponent. The relation between this exponent, frequency, and tank size is calculated for cylindrical enclosures from Daniels' acoustic theory. Daniels' solution is also used to find an average polytropic exponent for fluid capacitive circuits subjected to rectangular pulses of up to 8-sec duration.

Frequency response tests with finite amplitude are performed on fluid RCR circuits to determine the correspondence between the theory and the capacitance measured on lumped parameter circuits. The calculated data fall within 20 percent of the theory for circuits without through-flow.

Tests with small amounts of through-flow show only slight differences. The tendency is for through-flow to maintain isothermal conditions at frequencies above those that occur without through-flow.

14. KEY WORDS	LINK A		LINK B		LINK C	
	ROLE	WT	ROLE	WT	ROLE	WT
Fluidic capacitance	8	3				
Fluidic circuits	8	3				
Polytropic exponent						

AD

DA-1T61102A33B
AMCMS Code: 501B.11.71200
HDL Proj: 3FL31

HDL-TM-71-35

FLUERICS 31. THE TRANSITION FROM ISOTHERMAL TO ADIABATIC CAPACITANCE IN CYLINDRICAL ENCLOSURES

by

Silas Katz

Edgar Hastie

December 1971

U.S. ARMY MATERIEL COMMAND

HARRY DIAMOND LABORATORIES

WASHINGTON, D.C. 20438

ABSTRACT

The capacitance of enclosed volumes depends on the polytropic exponent. The relation between this exponent, frequency, and tank size is calculated for cylindrical enclosures from Daniels' acoustic theory. Daniels' solution is also used to find an average polytropic exponent for fluid capacitive circuits subjected to rectangular pulses of up to 8-sec duration.

Frequency response tests with finite amplitude are performed on fluid RCR circuits to determine the correspondence between the theory and the capacitance measured on lumped parameter circuits. The calculated data fall within 20 percent of the theory for circuits without through-flow.

Tests with small amounts of through-flow show only slight differences. The tendency is for through-flow to maintain isothermal conditions at frequencies above those that occur without through-flow.

BLANK PAGE

CONTENTS

ILLUSTRATIONS

NOMENCLATURE

a – radius of cylinder, m.

C_p – specific heat at constant pressure, joule/kg-°K

C – capacitance, m^5/kN

C_1 – constant of integration

C_2 – constant of integration

D – diameter of cylinder, m

F – frequency radius parameter

$|G(j\omega)|$ – amplitude density function for rectangular pulse

H – frequency circuit parameter $[\omega RC/(1 + R/R_L)]$

j – $\sqrt{-1}$

J_0 – Bessel function of the first kind of zeroth order

J_1 – Bessel function of the first kind of first order

K_1 – constant

k – thermal conductivity, joule/m-sec-°K

ℓ – length of cylinder, m

n – polytropic exponent

P – enclosure pressure, kN/m^2 absolute

P_1 – enclosure pressure amplitude, kN/m^2

P_0 – fluid circuit enclosure pressure, kN/m^2

P_i – supply pressure, kN/m^2

P_r – reference pressure, kN/m^2

Pr. – Prandtl's Number

Q_i – inlet volume flow, m^3/sec

Q_0 – outlet volume flow, m^3/sec

r – radial dimension, m

R – inlet resistor, $kN\text{-}sec/m^5$

R_L - load resistor, kN-sec/m^5

S_m - magnitude sensitivity factor

S_ϕ - phase sensitivity factor

t - time, sec

τ - pulse duration, sec

T - temperature, °K

T_1 - temperature amplitude, °K

T_{1_a} - average temperature amplitude, °K

u - axial velocity, m/sec

V - volume of enclosure, m^3

x - axial dimension, m

Y_0 - Bessel function of second kind of zeroth order

α - pressure amplitude parameter ($P_1^2 / \rho C_p$), °K

β - frequency parameter ($j \omega P_r / \mu$), m^{-2}

γ - ratio of specific heats

τ - tank circuit time constant, sec

ω - angular frequency, rad/sec

μ - kinematic viscosity, m^2/sec

ρ - density, kg/m^3

ρ_r - reference density, kg/m^3

1. INTRODUCTION

It is well known that the capacitance of gas-filled volumes depends on the thermodynamic process in the gas. Reference books[1,2] often refer qualitatively to isothermal capacitance for "slow" processes and adiabatic capacitance for "fast" processes. These relative terms are sufficient in some cases. Other cases require more precise information. This information is available but is not well known.

Daniels[3] provides analytical solutions for the capacitance of spheres, infinitely long circular cylinders, and long narrow rectangular boxes as a function of frequency and dimensions. These solutions are valid throughout the entire range from isothermal to adiabatic conditions. The fluid signals are acoustic, i.e., of small amplitude, sinusoidal, and without steady flow. Biagi and Cook[4] extend the analysis to the case of a finite length circular cylinder. In this case the solution is in the form of an infinite series. Gerber[5,6] shows that the capacitance throughout the transition from isothermal to adiabatic flow also depends on the driving and load impedances to the chamber, whereas the previous papers[3,4] apply only to a zero impedance driver. In the calibration of microphones the infinite (rigid piston) is appropriate. However, the zero impedance driver is a better approximation for most of the circuits that occur in fluid control systems. Actually Iberall[7], Nichols[8] and Brown[9] in their investigations of fluid transmission lines derive a capacitance that is identical to Daniels' formulation[3] for a cylindrical enclosure. Schaedel[10] solves for the capacitance in rectangular fluid transmission lines of various aspect ratios. The results agree with Daniels[3] for the special case of a narrow (high aspect ratio) enclosure.

The purpose of this investigation is to compare the transition of capacitance predicted by the acoustic theory and that measured in a typical lumped parameter fluid circuit with and without a steady flow.

2. FLUID TANK CAPACITANCE

Fluid capacitance, which is the most common time-dependent fluid circuit component, is a consequence of fluid continuity.

Consider the rigid-walled chamber of volume V, shown in figure 1. The chamber has two ports. A mass flow (density-volume flow product), Q_1, enters one port, and a mass flow

---

[1] Gibson, J. E. and F. B. Tuteur, "Control System Components," McGraw-Hill Book Company, 1958, p. 447.

[2] Zalmanzon, L. A., "Components for Pneumatic Control Instruments," Pergamon Press, 1965, p. 160.

[3] Daniels, F. B., "Acoustical Impedance of Enclosures," Journal of the Acoustical Society of America, Volume 19, November 4, p. 569, July, 1947.

[4] Biagi, F. and R. K. Cook, "Acoustic Impedance of a Right Circular Cylindrical Enclosure," Journal of the Acoustical Society of America, Volume 26, Number 4, p. 506, July 1954.

[5] Gerber, H., "Acoustic Properties of Fluid-Filled Chamber at Infrasonic Frequencies in the Absence of Convention," Journal of the Acoustical Society of America, Volume 36, p. 1427, 1964.

[6] Gerber, H., "Transient and Sinusoidal Thermal Diffusion, Convection, and Related Infrasonic Pressure Changes in Enclosed, Homogeneous Fluids," U. S. Naval Ordnance Lab., Technical Report 62-94, 1963.

[7] Iberall, A. S., "Attenuation of Oscillatory Pressures in Instrument Lines," Journal of Research, National Bureau of Standards, Volume 45, July, 1950, R.P. 2115.

[8] Nichols, N. B., "The Linear Properties of Pneumatic Transmission Lines," ISA Transactions, Volume I, No. 1, January, 1962.

[9] Brown, F. T., "Pneumatic Pulse Transmission with Bistable-Jet Relay Reception and Amplification," ScD Thesis, MIT, May, 1962.

[10] Schaedel, H., "A Theoretical Investigation of Fluidic Transmission Lines with Rectangular Cross Section," Third Cranfield Fluidics Conference, Paper K3, May, 1968.

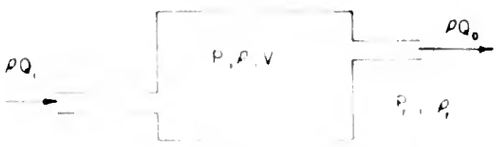

Figure 1. Fluid Tank Capacitance

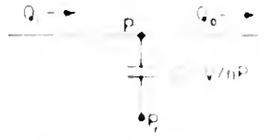

Figure 2. Equivalent Circuit for Tank Capacitance

ρQ_0 exits through the other. Within the chamber, the total pressure is p, and the density is ρ, while outside the chamber, reference conditions P_r and ρ_r exist. Although the density in the tank is time-dependent, we assume that it is independent of position. Now if we equate the net mass flow to the time rate of change of mass stored in the chamber, the result is:

$$\rho [Q_i - Q_0] = V \frac{d}{dt} [\rho - \rho_r] \tag{1}$$

Equation 1 provides a relation between the volume flows (Q_i, Q_0) and the density. However, the assumed signal variables for the fluid circuit are volume flow and total pressure. To express equation 1 in terms of the signal variables we use the polytropic process formulation

$$P = K_1 \rho^n \tag{2}$$

where n is the polytropic exponent and K_1 is a constant. The application of equation 2 to equation 1 yields

$$Q_i - Q_0 = \frac{V}{n P} \frac{d}{dt} [P - P_r] \tag{3}$$

Since volume flow is the through variable and pressure drop, the across variable, the proportionality constant, V/nP, equals the capacitance, C of the chamber. Figure 2 shows an equivalent electrical circuit that represents equation 3.

One terminal of the capacitance is at the instantaneous tank pressure, and the other is at the reference pressure. Since the reference pressure is a mathematical concept, it is not possible to connect physically to this terminal.

The magnitude of the capacitance depends on the value of the polytropic exponent. When the process is isothermal, n = 1.0, and when it is adiabatic, n = 1.4. The exponent can take on any value between these extremes. To calculate the exponent requires an equation of state. If we assume an ideal gas, the differential form of the state equation is:

$$\frac{dP}{P} = \frac{d\rho}{\rho} + \frac{dT}{T} \tag{4}$$

where T is the temperature of the gas. Now the elimination of density between equation 2 and equation 4 results in

$$n = \frac{1}{1 - \left(\frac{P}{T}\right)\left(\frac{dT}{dP}\right)} \tag{5}$$

To evaluate the polytropic exponent from equation 5 requires a relation between temperature and pressure. Some special solutions of the thermal energy equation yield this relation. The polytropic exponent then follows from the combination of these solutions with equation 5.

2.1 Daniels' Solution for Cylindrical Enclosures with Sinusoidal Signals

To demonstrate the calculation of the polytropic exponent and to get a better physical understanding of the problem, we present a modified development of Daniels' solution for cylindrical enclosures subjected to sinusoidal signals. Figure 3 shows the coordinates of the cylinder.

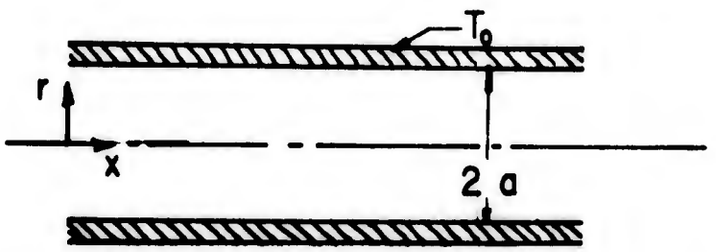

Figure 3. Coordinate System for Cylindrical Tank

If frictional heating is negligible and the axial velocity is large compared to the radial velocity, the thermal energy equation in cylindrical coordinates is:

$$\rho C_p \left[\frac{\partial T}{\partial t} + u \frac{\partial T}{\partial x}\right] = \frac{\partial P}{\partial t} + u \frac{\partial P}{\partial x} + \frac{k}{r}\left[\frac{\partial}{\partial r}\left(r \frac{\partial T}{\partial r}\right)\right] + K \frac{\partial^2 T}{\partial x^2} \tag{6}$$

where u is the axial velocity, t is time, k is the thermal conductivity of the gas, and C_p is the specific heat at constant pressure. The left side of equation 6 represents the internal energy in the gas. The first two terms on the right side of equation 6 indicate the compression work, and the last two terms, the heat conduction. When there is no component of steady axial flow, and the temperature is not a function of axial position (infinitely long cylinder), equation 6 reduces to:

$$\rho C_p \frac{\partial T}{\partial t} = \frac{\partial P}{\partial t} + \frac{k}{r}\left[\frac{\partial}{\partial r}\left(r \frac{\partial T}{\partial r}\right)\right] \tag{7}$$

Equation 7 transforms to an ordinary differential equation if we let:

$$T(r) = T_1(r) \exp[j \omega t] \tag{8a}$$

$$P = P_1 \exp[j \omega t] \tag{8b}$$

where T_1 and P_1 are the amplitudes of temperature and pressure, ω is the angular frequency, $j = \sqrt{-1}$, and temperature is a function of r. The substitution of equation 8 into equation 7 yields:

$$\frac{d^2 T_1}{d r^2} + \frac{1}{r} \frac{d T_1}{d r} = \beta^2 (T_1 - \alpha) \tag{9}$$

where

$$\beta^2 = \frac{j \omega \rho C_p}{k} = \frac{j \omega Pr}{\nu}, \quad \alpha = \frac{P_1}{\rho C_p}$$

and Pr. is Prandtl's number and ν is the kinematic viscosity. For the usual case of isothermal walls the boundary conditions for equation 9 are:

$$r = 0, \quad \frac{d T_1}{d r} = 0 \tag{10a}$$

$$r = a, \quad T_1 = 0 \tag{10b}$$

where a is the cylinder radius.

The solution of equation 9 is:

$$T_1 = C_1 J_0 (j \beta r) + C_2 Y_0 (j \beta r) + \alpha \tag{11}$$

where J_0 is a Bessel function of the first kind of zeroth order, Y_0 is a Bessel function of the second kind of zeroth order, and C_1 and C_2 are the constants of integration. The evaluation of the integration constants with the given boundary conditions leads to the following expression for the temperature distribution.

$$\frac{T_1}{\alpha} = 1 - \frac{J_0 (j \beta r)}{J_0 (j \beta a)} \tag{12}$$

Equation 12 gives the magnitude and phase of the temperature amplitude distribution within the cylinder. Calculation of this distribution is somewhat simpler if we select a frequency-radius parameter $F = \beta a / j^{1/2} = a(\omega Pr. \rho)^{1/2}$. Then equation 12 becomes:

$$\frac{T_1}{\alpha} = 1 - \frac{J_0 \left(j^{3/2} F \frac{r}{a}\right)}{J_0 (j^{3/2} F)} = 1 - \frac{Ber_0 \left(F \frac{r}{a}\right) + j Bei_0 \left(F \frac{r}{a}\right)}{Ber_0 (F) + j Bei_0 (F)} \tag{13}$$

Figure 4a shows the temperature amplitude distribution, and figure 4b shows the temperature phase distribution for various values of the parameter F. When F = 0 (zero frequency or zero radius), the temperature amplitude is uniform at the wall temperature, and the temperature leads the pressure by 90 degrees. As F increases, the temperature amplitude is maximum on the axis until F reaches approximately 5.0. Thereafter, the maximum occurs along a circular cylindrical shell. Ultimately, when F > 20 the gas asymptotically approaches a uniform temperature ($T_1 / \alpha = 1$) except for the singularity at the isothermal walls where $T_1 / \alpha = 0$. The phase distribution of temperature follows an inverse pattern in which the phase lead decreases until the temperature and pressure are in phase at high values of F (> 20).

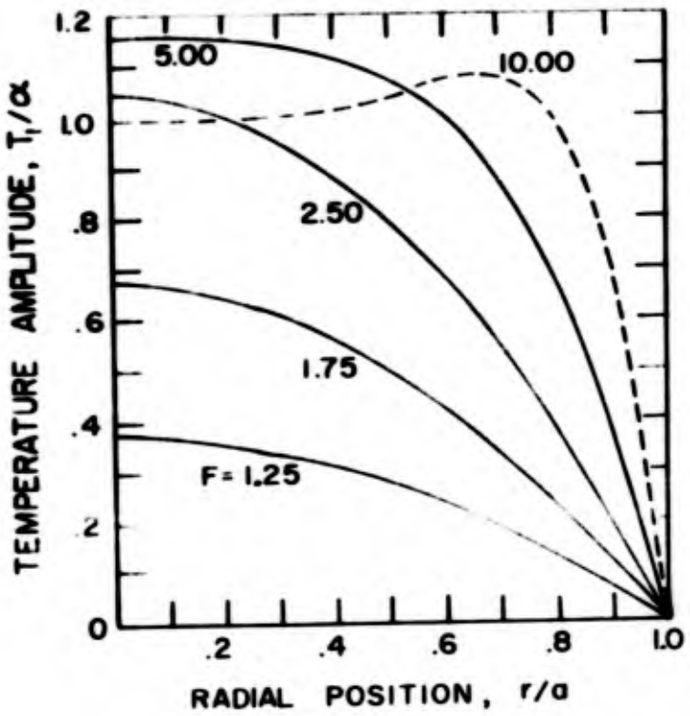

Figure 4 (a) Temperature Amplitude Distribution

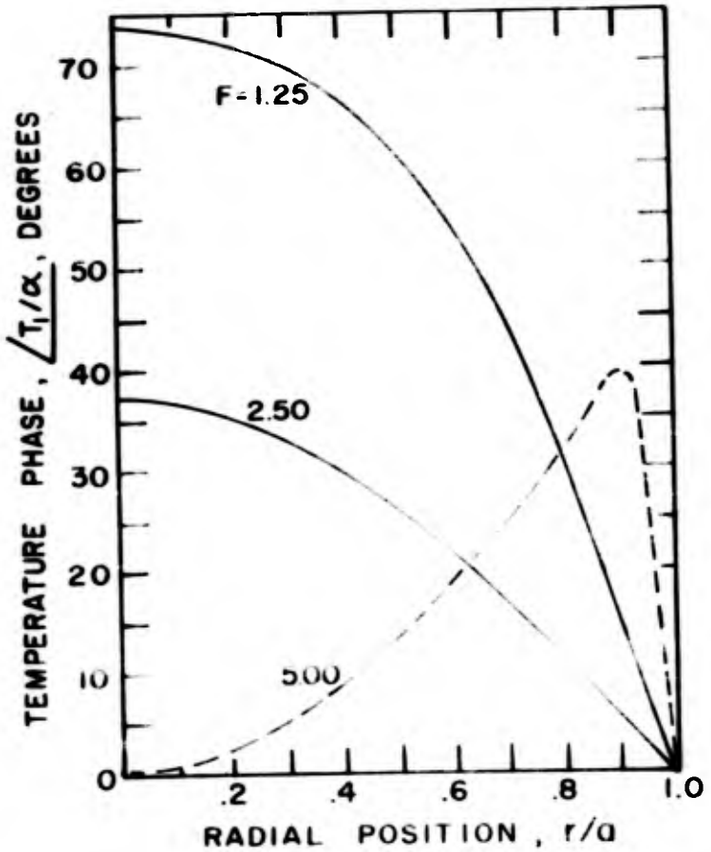

Figure 4 (b) Temperature Phase Distribution

To obtain a single representative value of the polytropic exponent we must average the temperature distribution. The average temperature, $\bar{T}_1$, for the cylindrical enclosure is:

$$\frac{\bar{T}_1}{\alpha} = \frac{2\pi \int_0^a (T_1/\alpha)\, r\, dr}{\pi a^2} \tag{14}$$

The substitution of equation 13 into equation 14 and subsequent integration leads to:

$$\frac{\bar{T}_1}{\alpha} = \left[1 - \frac{2 J_1 (j^{3/2} F)}{j^{3/2} F J_0 (j^{3/2} F)}\right] \tag{15}$$

Now if we assume that $dT/dP = \bar{T}_1/P_1$ and apply the ideal gas law $P = \rho C_p T(1 - 1/\gamma)$, where γ is the ratio of specific heats, equation 5 becomes:

$$n = \frac{1}{1 - (1 - 1/\gamma)\, \bar{T}_1/\alpha} \tag{16}$$

The replacement of $\bar{T}_1/\alpha$ in equation 16 by the expression given in equation 15 produces:

$$n = \frac{\gamma}{1 + \dfrac{2(\gamma - 1)}{j^{3/2} F} \dfrac{J_1 (j^{3/2} F)}{J_0 (j^{3/2} F)}} \tag{17}$$

The formulation of the polytropic exponent given in equation 17 is the ratio of isothermal capacitance to shunt admittance as determined by Brown[9] for the fluid transmission line. Figure 5 is a plot of equation 17 and shows the continuous transition from isothermal to adiabatic as the parameter F increases. To display the frequency dependence more readily, figure 6 shows a non-normalized representation of equation 17 for the case of air at standard conditions. Figure 6 is a log-log plot with frequency as ordinate, chamber diameter as abscissa, and polytropic exponent as parameter. At constant polytropic exponent the graph consists of straight parallel lines with a slope of -2. The regions beneath the n = 1.05 line and above the n = 1.35 line are essentially isothermal and adiabatic respectively. Thus, for example, a 10-mm diameter chamber operating at 0.2 Hz is practically isothermal whereas the same chamber operating at 1.8 Hz has a polytropic exponent of 1.2.

The above development applies to long chambers ($\ell/D = \infty$). Biagi and Cook[4] develop the relation between the polytropic exponent and the ratio of volume to surface area for finite length cylindrical enclosures. They show that the results between the infinite length cylinder and one where $\ell/D = 2.37$ are not too different. Heat transfer to the end plates of finite length cylinders tends to reduce the average temperature amplitude and thereby increases the polytropic exponent. However, the difference in polytropic exponent between ℓ/D ratios of 2.37 and ∞ is less than 2 percent.

[4] Biagi, F. and R. K. Cook, "Acoustic Impedance of a Right Circular Cylindrical Enclosure," Journal of the Acoustical Society of America, Volume 26, Number 4, p. 506, July 1954.

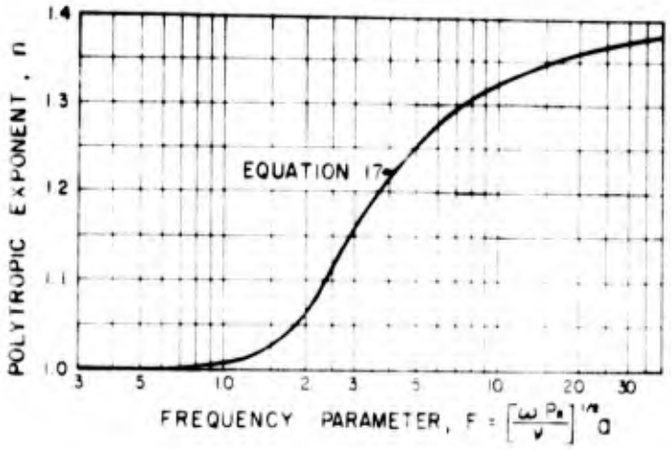

Figure 5. Frequency Dependence of Polytropic Exponent

2.2 Cylindrical Enclosures with a Rectangular Pulse Signal

The previous section shows the frequency dependence of the polytropic exponent. Fluid circuits, however, often operate with pulse type signals rather than sinusoidal waves. As a result, an appropriate value of the polytropic exponent for pulse signals is desirable. To obtain the appropriate value we use the frequency spectrum of the pulse signal in conjunction with the frequency spectrum of the polytropic exponent (equation 17).

We consider the case of a single rectangular pulse (fig. 7a) of width t_p, and unit height. The amplitude density function, $|G(j\omega)|$, for the rectangular pulse is from Kuo:[11]

$$|G(j\omega)| = t_p \left| \frac{\sin \omega t_p/2}{\omega t_p/2} \right| \tag{18}$$

Figure 7b shows the amplitude density spectrum for the rectangular pulse. The spectrum consists of an infinite number of loops of width $2\pi/t_p$. The loops become progressively smaller as frequency increases. This rectangular pulse signal is applied outside the enclosure. Since we require the amplitude spectrum within the enclosure we multiply the pulse spectrum by the spectrum for an RC circuit. The formulation for the average polytropic exponent is then:

$$\bar{n} = \frac{\int_0^\infty \frac{1}{\sqrt{1+\omega^2\tau^2}} |G(j\omega)| \, n \, d\omega}{\int_0^\infty \frac{1}{\sqrt{1+\omega^2\tau^2}} |G(j\omega)| \, d\omega} \tag{19}$$

[11] Kuo, B. C., "Analysis and Synthesis of Sampled-Data Control Systems," Prentice-Hall, 1963

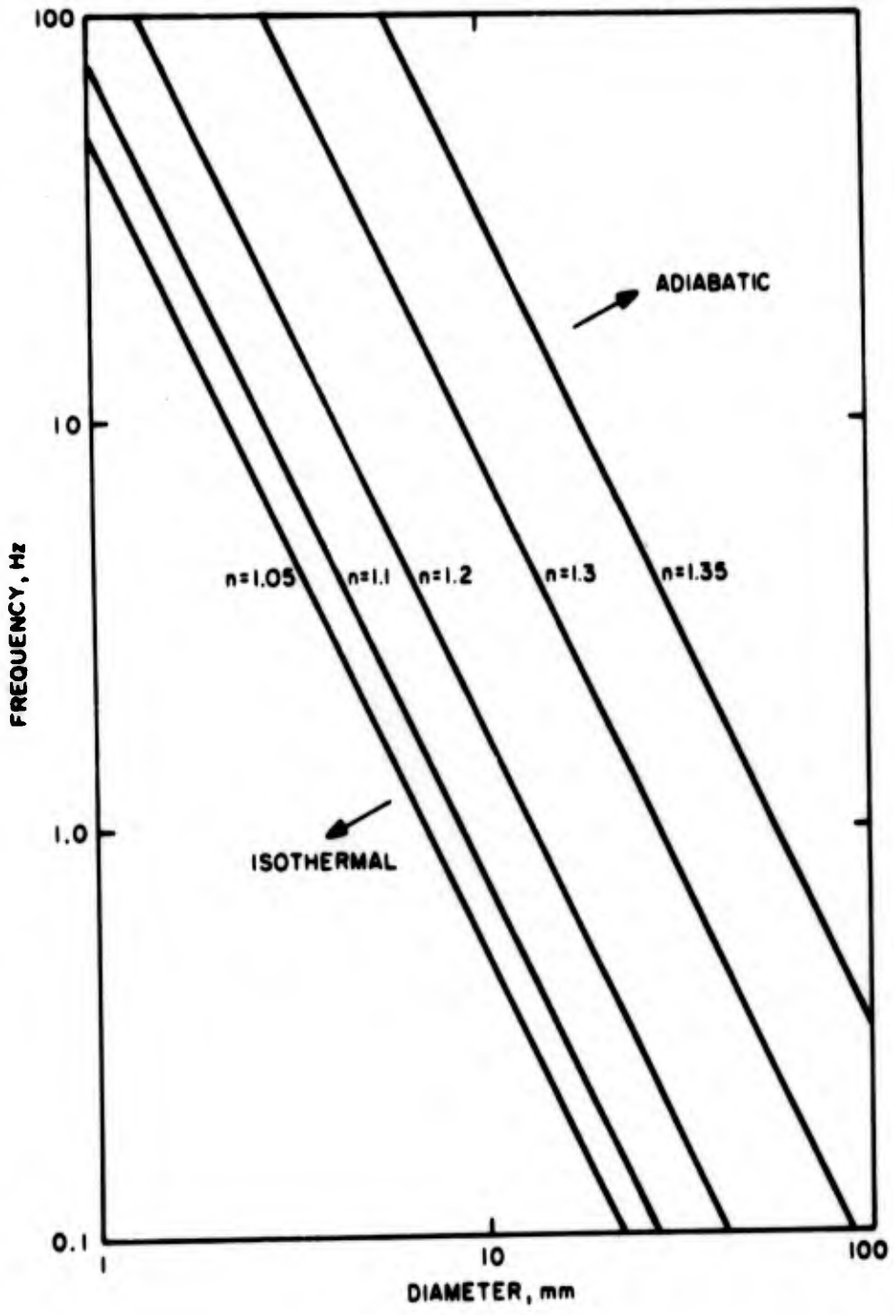

Figure 6. Design Chart of Polytropic Exponent for Sinusoidal Signals

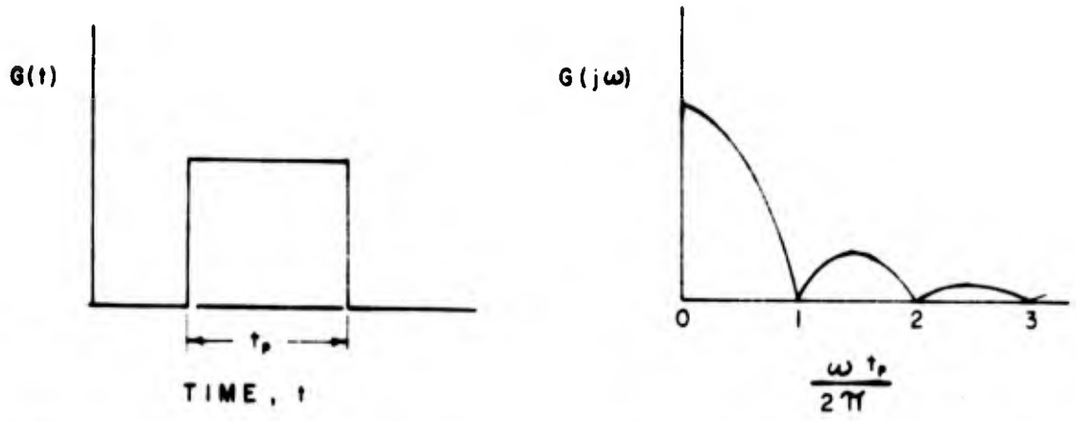

Figure 7. Amplitude Spectrum for Retangular Pulse

where τ is the time constant of the fluid circuit. We evaluate the integrals of equation 19 by numerical methods. In the computation the upper limit for the integrals is $8\pi/t_p$ (4 loops). The error due to the neglect of frequencies above this is less than 2 percent. Figures 8a, b and c show the average polytropic exponent as a function of pulse width for various enclosure diameters when the time constant is 0.01, 0.1, and 10.0 sec, respectively. Short pulses (less than 0.05 sec) are essentially adiabatic. The transition from adiabatic to isothermal is most rapid for small diameter tanks. Large diameter tanks remain almost adiabatic even for long pulses. The time constant of the tank is important only when the pulse duration is short.

3. FLUID LUMPED-PARAMETER RCR CIRCUIT

The theory presented for enclosures was developed specifically to improve the accuracy of microphone calibration (using a piston-driven chamber) and has yielded excellent correspondence with experimental results. The purpose of this study is to determine the applicability of the theory to a typical lumped-parameter fluid circuit. For this reason, we consider the simple fluid circuit shown in figure 9.

The circuit consists of a supply chamber, a test chamber, and two resistors, R and R_L. The capillary resistor R connects the supply and test chamber. The load resistor R_L connects the test chamber to a reference pressure. When R_L is infinite, there is no steady flow through the test tank and the circuit is known as a blank chamber circuit. For finite values of R_L there is a steady flow through the test chamber and we call these through-flow circuits.

Figure 10 shows the electrical equivalent circuit for the fluid RCR circuit for frequencies low enough that inertance can be neglected (i.e., well below the resonant frequency of the tank).

In these tests we imposed a sinusoidal pressure signal on the supply tank and measured the corresponding pressure in the test tank. The complex relation between test and supply pressures is:

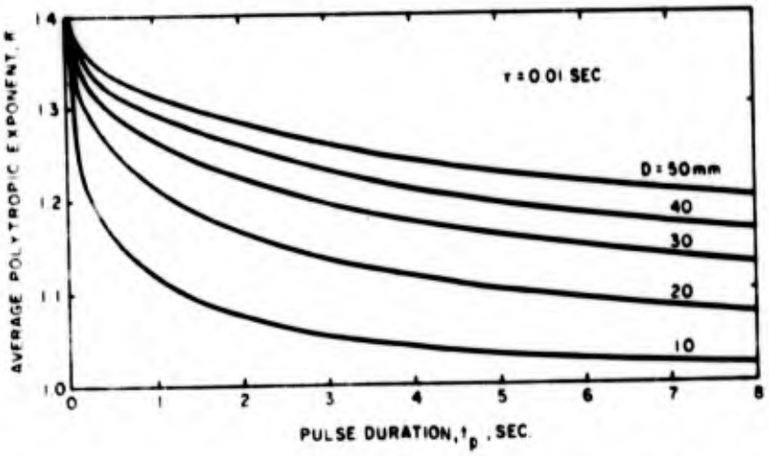

Figure 8 (a). Average Polytropic Exponent for Rectangluar Pulses (τ=0.01 sec)

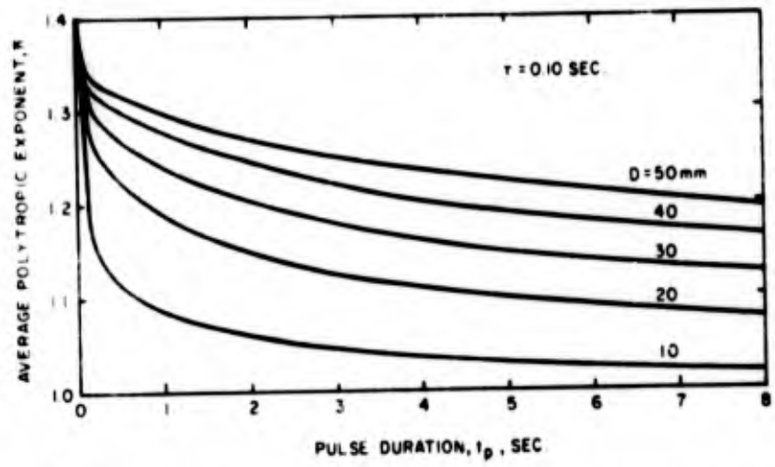

Figure 8 (b). Average Polytropic Exponent for Rectangular Pulses (τ=0.10 sec)

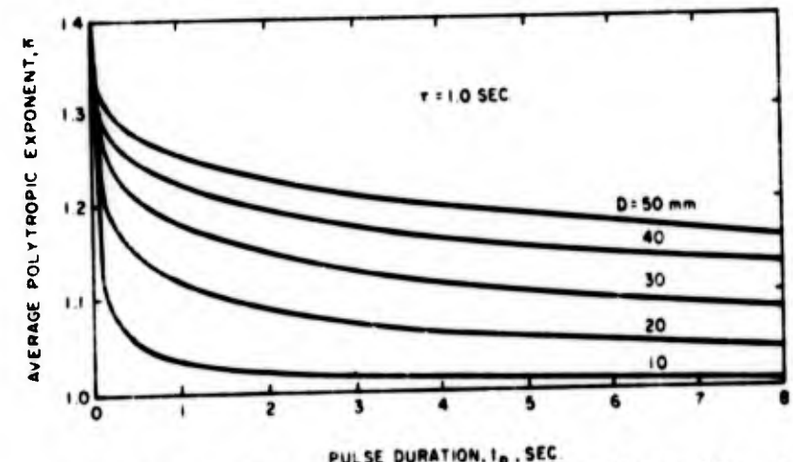

Figure 8 (c). Average Polytropic Exponent for Retangular Pulses (τ=1.00 sec)

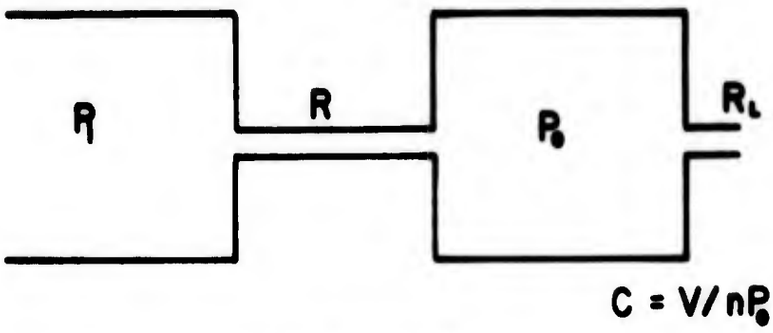

Figure 9. Fluid RCR Circuit

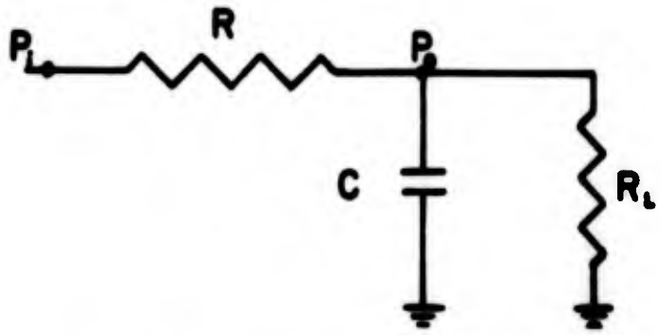

Figure 10. Equivalent Electrical RCR Circuit

$$\frac{P_0(j\omega)}{P_i(j\omega)} = \frac{1}{(1 + R/R_L) + j\omega RC} \tag{20}$$

The objective of the tests was to calculate the capacitance as a function of frequency. Magnitude and phase measurements of the pressures in the tanks (P_i and P_0) provide two sets of data for the calculation. Thus, from equation 20:

$$\omega RC = \sqrt{\left[\frac{P_i(j\omega)}{P_0(j\omega)}\right]_m^2 - (1 + R/R_L)^2} \tag{21a}$$

$$\omega RC = (1 + R/R_L) \tan\left[\frac{P_0(j\omega)}{P_i(j\omega)}\right]_\phi \tag{21b}$$

where the subscript m denotes the magnitude measurement, and the subscript ϕ denotes the phase measurement.

To indicate the relation between errors in measurement and the resulting error in capacitance calculation we define the following error sensitivity factors.

$$S_{|P_1 - P_0|, |P_1 - P_0|} = \frac{d|C - C|}{d|P_1 - P_0|, |P_1 - P_0|} \tag{22a}$$

$$S_{\angle(P_1 - P_0), \angle(P_1 - P_0)} = \frac{d|C - C|}{d\angle(P_1 - P_0), \angle(P_1 - P_0)} \tag{22b}$$

The sensitivity factors for the functions given in equation 21 are:

$$S_{|\ |} = 1 + 1/H^2 \tag{23a}$$

$$S_{\angle\ } = \frac{H^2 + 1}{H} \tan^{-1} H \tag{23b}$$

where the frequency-circuit parameter $H = \omega RC/(1 + R/R_L)$. Figure 11 shows the relation between the sensitivity factors of equation 23 and the parameter, H. The magnitude sensitivity factor is large at small values of H and decreases monotonically toward unity as H increases. At $H = 0.2$, the magnitude sensitivity is 26. This means, for example, that a 10 percent error in the measurement of magnitude ratio will result in a 260 percent error in the calculated capacitance. When $H = 6$ the magnitude sensitivity is 1.03 and a 10 percent measurement error only causes a 10.3 percent calculation error. The phase sensitivity factor, on the other hand, is near unity at small values of H and increases to 8.7 when H increases to 6.0. To limit the error sensitivity to a maximum of 1.5 over the entire range we might make phase measurements when $H \leq 1.2$ and amplitude measurements when $H \geq 1.2$. One of the difficulties with this plan, as shown in section 4.1, is that the error in phase measurements increases as H decreases. Thus, although the error in phase measurement is not amplified by calculation, it is sizeable enough of itself to cause a considerable error in the capacitance. For this reason, we introduce a third function for the computation of capacitance.

In the third or differential method the vector difference of two signals is measured directly. To demonstrate the rationale of this method we rewrite equation 20 in the following way:

$$\frac{P_1(j\omega) - (1 + R/R_L) P_0(j\omega)}{P_0(j\omega)} = j\omega RC \tag{24}$$

The function in equation 24 has a magnitude of ωRC and a constant phase angle of 90 degrees. The result of equating the magnitude of each side of equation 24 is:

$$\omega RC = \frac{|P_1(j\omega) - (1 + R/R_L) P_0(j\omega)|}{|P_0(j\omega)|} \tag{25}$$

To calculate capacitance from equation 25 we must measure the amplitude of the vector difference between supply pressure (P_1) and the product of $(1 + R/R_L)$ and tank pressure (P_0). This is the numerator of the right hand side of equation 25. The denominator is merely the amplitude of the tank pressure alone. The sensitivity of the differential method is unity throughout the entire range of H.

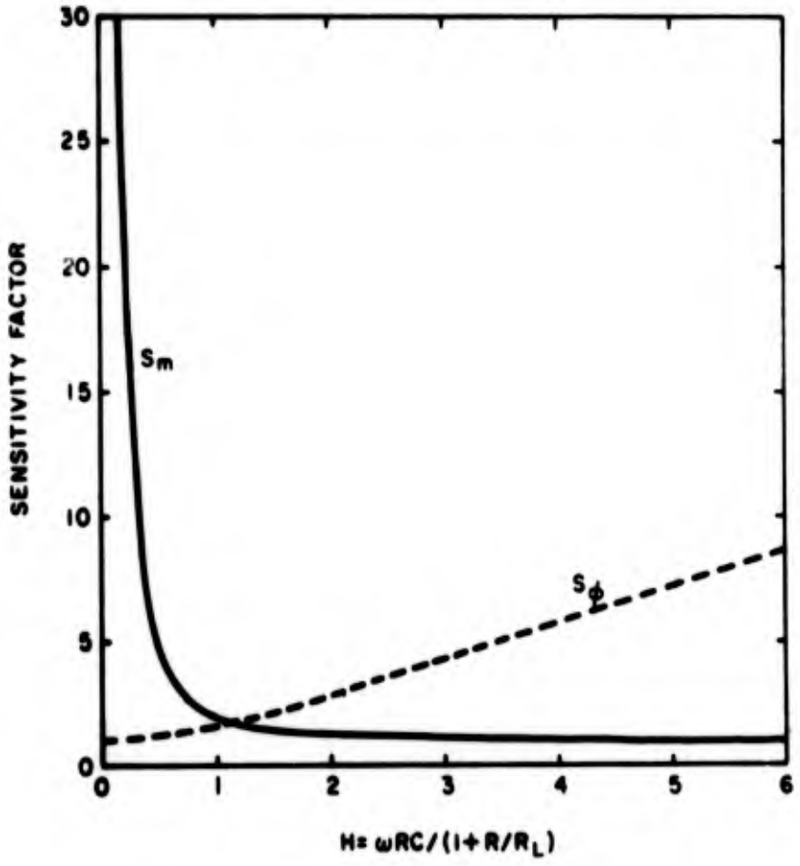

Figure 11. Error Sensitivity of RCR Function

4. EXPERIMENTAL PROGRAM

Figure 12 shows a schematic drawing of the experimental set-up. An electronic sinusoidal wave generator drives a fluid signal generator which in turn provides a fluid sinusoidal signal to the fluid RCR circuit. The air supply to the fluid signal generator passes through a filter, a pressure regulator, and 15.25 m of 0.475 cm. diameter copper tubing to minimize air temperature variations. Variable reluctance pressure transducers convert the pressures at the entrance to the RCR circuit (P_i) and in the test chamber (P_0) to electrical signals. The following section describes the measurement of the electrical signals.

4.1 Measurement Techniques

Equations 21a, 21b, and 25 indicate that to calculate the capacitance of the test chamber requires measurements of either magnitude or phase of the difference between two phasors. In this program the capacitance was obtained by all three methods.

1. Magnitude Techniques

The magnitude of the input and output sinusoidal function was measured with

(a) Peak to Peak Voltmeter

(b) RMS Voltmeter

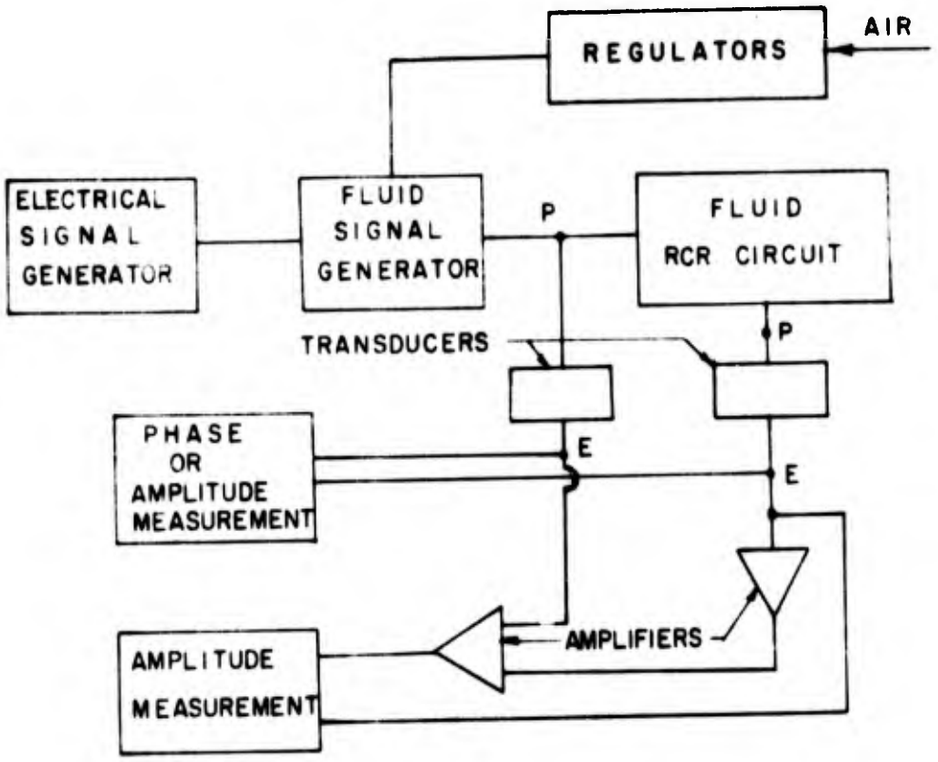

Figure 12. Schematic of Experimental Set-Up

(c) XY Recorder or Storage Oscilloscope

(d) Digital Voltmeter

Each of these instruments causes some difficulties in the present application. The peak to peak and RMS meters are not accurate at frequencies below 5 Hz, and these frequencies are essential in the present experiment. Electro-mechanical XY recorders, on the other hand, have significant dynamic effects above 1 Hz, and besides neither recorders nor storage oscilloscopes provide sufficient resolution. The problem with the digital voltmeter is that it is a dc device and is difficult to read even at low frequencies. For these reasons amplitude measurements below 5 Hz are accurate only to within 10 percent.

2. Phase Techniques

The techniques for measuring phase are

(a) Phasemeter

(b) Electronic Counter

(c) Electrical Simulation

(d) Lissajous Pattern

(e) Transportation Delay Generator

Here again each method has some shortcomings. The phasemeter does not operate at low frequencies, and the counter has problems associated with a consistent triggering level. In

the electrical simulation method, an electrical RCR circuit, which consists of variable R and C components, is adjusted until its response is the same as the fluid RCR circuit. The difficulty in this case occurs in the detection of a null between the circuits. One of the most satisfactory methods overall is the Lissajous pattern method. The input and output signals are plotted against each other on a recorder or storage oscilloscope. In the range of phase shifts above 10 degrees this method is accurate to within 10 percent. However at small phase angles there is a systematic error in the measurements due to small differences in the transducer calibration. Even when this error is corrected, there remains considerable uncertainty because of the width of the trace on the storage oscilloscope. Thus small phase angles may be only within 30 or 40 percent of the true phase. In the transportation delay method the input signal passes through an adjustable pure time delay. The delay time required to achieve a straight line Lissajous display of the output and delayed input is a measure of the phase difference. The precise point of null, however, is not sharp and depends to some extent on the observer. The accuracy of this method is comparable to the Lissajous method.

3. Difference Techniques

There are two difference techniques:

(a) Differential Transducer

(b) Operational Amplifiers

The differential transducer method has two limitations. One is that the calibration is not always exactly the same in each direction. The other is that it requires additional fluid lines in the fluid circuit and in that respect alters the magnitude of the fluid response. In addition this method is applicable only to blank chamber tests. The operational amplifier method (Figure 12) consists of multiplying the output signal by $(1 + R/R_L)$ and then using another electronic amplifier to take the difference of this and the input signal. The amplitude of these signals is measured from the oscilloscope trace, and thus the accuracy depends again on the resolution of such a reading. Under these circumstances the accuracy of the measurements is probably no better than about 10 percent. Since measurements by the magnitude, phase and difference methods have about the same accuracy, consideration of the sensitivity factors is necessary. These factors favor the difference method as the most accurate means of calculating the capacitance.

4.2 Fluid Test Circuits

This investigation deals with two types of fluid circuits. In blank chamber circuits, there is only a single small opening into the cylindrical test enclosure. A capillary resistance connects the supply chamber to the test chamber through this opening. In the other fluid circuit, the through flow circuit, the test chamber has another small opening on the opposite flat surface which permits flow to pass from the supply chamber through a capillary resistor to the test chamber and then from the test chamber through an orifice to atmospheric pressure. Table I lists the dimensions of the cylindrical test chambers, the magnitude of the capillary resistance in the blank chamber tests and the measuring techniques used.

TABLE I. Blank Chamber Tests.

Volume cc.	Diameter cm	Length cm	R kN-sec/m^5	Measurement Technique
164	4.92	8.48	.105(10)^6	Amplitude Phase-Lissajous
164	4.92	8.48	.445(10)^6	Phase-Transport Phase-Simulation Difference
164	2.38	36.7	.105(10)^6	Amplitude Phase-Lissajous
164	2.38	36.7	.445(10)^6	Phase-Transport Phase-Simulation Difference
16.4	2.38	3.67	.105(10)^6	Phase-Lissajous
16.4	2.38	3.67	.445(10)^6	Phase-Transport Phase-Simulation Difference
16.4	1.11	16.9	.445(10)^6	Phase-Transport Phase-Simulation Difference

In the blank chamber tests the cylindrical test enclosures had a volume of either 16.4 cc or 164 cc. The smaller volume was obtained with cylinder diameters of 1.11 cm and 2.38 cm, and corresponding lengths of 16.9 cm and 3.67 cm. The larger volume was obtained from 2.38 cm and 4.92 cm diameter cylinders which are 36.7 cm and 8.48 cm long, respectively. Twenty-five parallel capillary tubes provided linear resistances of either .105(10)^6 kN-sec/m^5 or .445(10)^6 kN-sec/m^5. For all the tests the average absolute pressure in the test enclosure was 106.8 kN/m^2, and the peak-to-peak amplitude of the input signal in the supply chamber was 1.38 kN/m^2.

Table II gives the pertinent information for the through flow circuit tests.

TABLE II. Through Flow Tests.

Volume = 2.95 (10)$^{-5}$ m^3 Length = 30.5 cm
Diameter = 1.11 cm Measuring Technique = Difference

Flow cc/sec	Velocity cm/sec	R kN-sec/m^5	R_L kN-sec/m^5
0	0	.105(10)^6	
35.8	38	.155(10)^6	.078(10)^6
73.6	76	.218(10)^6	.042(10)^6

The through flow tests were performed with a test enclosure is 1.11 cm in diameter and 30.5 cm long. In one test the chamber was blanked off, and the through flow was zero. The velocity of through flow in the other tests was either 38 cm/sec or 76 cm/sec. To attain these through flow velocities requires very small load resistance, and this leads to capillary tubes bundled together in parallel. A limitation occurs when the bundle size exceeds the cylinder diameter. For this reason an adjustable small size orifice was used as the load resistance in the through flow tests. Since the test level is fixed at the same dc and amplitude values as the blank chamber tests, the orifice resistance does not change appreciably during a test. However, the upstream capillary resistance does change as the through flow increases. This occurs because the pressure drop across these capillaries increases and the flow in the capillaries becomes turbulent. During the experiment, however, the magnitude of the capillary resistance remains essentially constant at the adjusted value.

4.3 Experimental Data

Figures 13, 14, 15 and 16 show the data from the blank chamber tests, and figure 17, the data from the through flow tests. In all the tests the data always falls within 20 percent of the capacitance predicted by using Daniels' long cylinder theory for the polytropic exponent (equation 17). There is a slight but well-defined difference between tests with different measuring techniques. For example the phase-transport method consistently produces lower values of the capacitance than the difference method. As expected from the sensitivity analysis, the phase method results become more divergent at the higher frequencies where the phase shift is large. The difference method, on the other hand, seems to have the largest discrepancies when the frequencies are small. This may be a function of the preciseness of the input and output transducers. At low frequencies we are subtracting amplitudes which are very nearly equal. If the transducers are not well matched in calibration, the largest errors would occur in this range.

The through flow tests use only the difference measuring technique. This facilitates the comparison between the tests and thereby shows the effects of through flow. In the present experiments the effect of the small through flow on the frequency dependence of fluid capacitance is relatively small if any difference exists. The data do show a slight tendency toward higher frequency transition as through flow increases. However this may be the result of experimental error rather than the result of an alteration in the temperature distribution. The error which causes the uncertainty may be in the measurement of the capillary associated with each value of through flow. This resistance is determined by measurement of the slope of the pressure drop-volume flow curve, and a small error could account for most of the observed discrepancy between through flow tests.

5. SUMMARY

Daniels' theory for the acoustic impedance of cylindrical enclosures has been examined in detail. The theory requires the derivation of the temperature distribution in the enclosure. The temperature distribution changes in both amplitude and phase when the frequency changes. The resulting expression for the polytropic exponent is identical to the shunt admittance correction factor given by Brown for fluid transmission lines. However the complex form of the exponent makes it difficult to utilize in a circuit application. As an aid to fluid circuit designers a log-log plot is given which shows at a glance the correct exponent for a particular application with sinusoidal signals. Daniels' solution was also utilized in the determination of an average polytropic exponent for circuits with rectangular pulse signals.

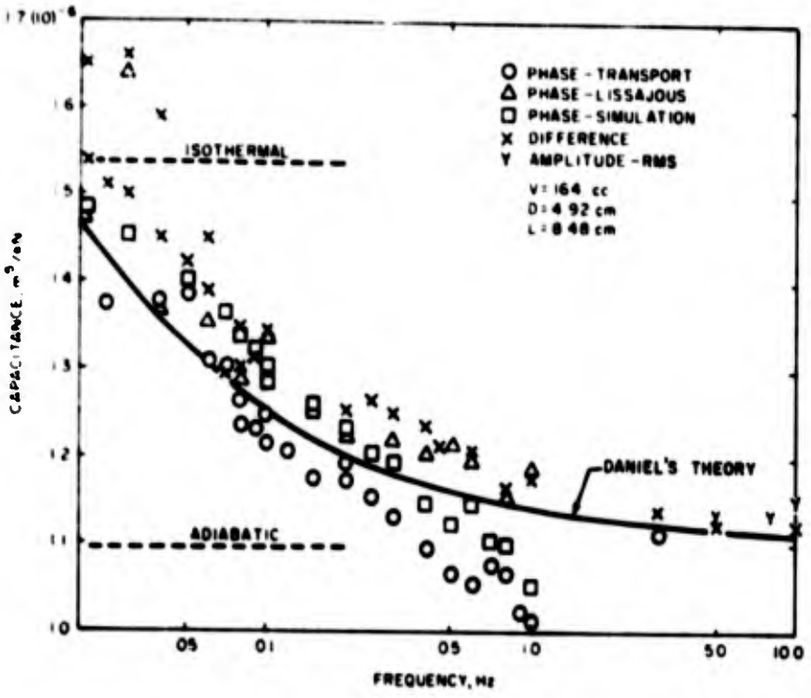

Figure 13. Capacitance vs. Frequency ($V = 1.64\ (10)^{-4}\ m^3$, $D = 4.92$ cm.)

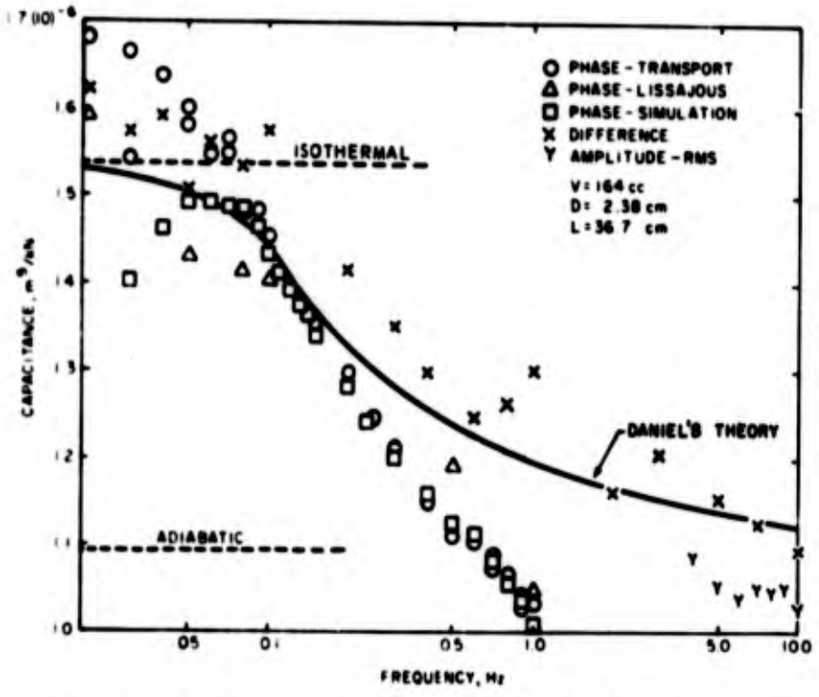

Figure 14. Capacitance vs. Frequency ($V = 1.64\ (10)^{-4}\ m^3$, $D = 2.38$ cm.)

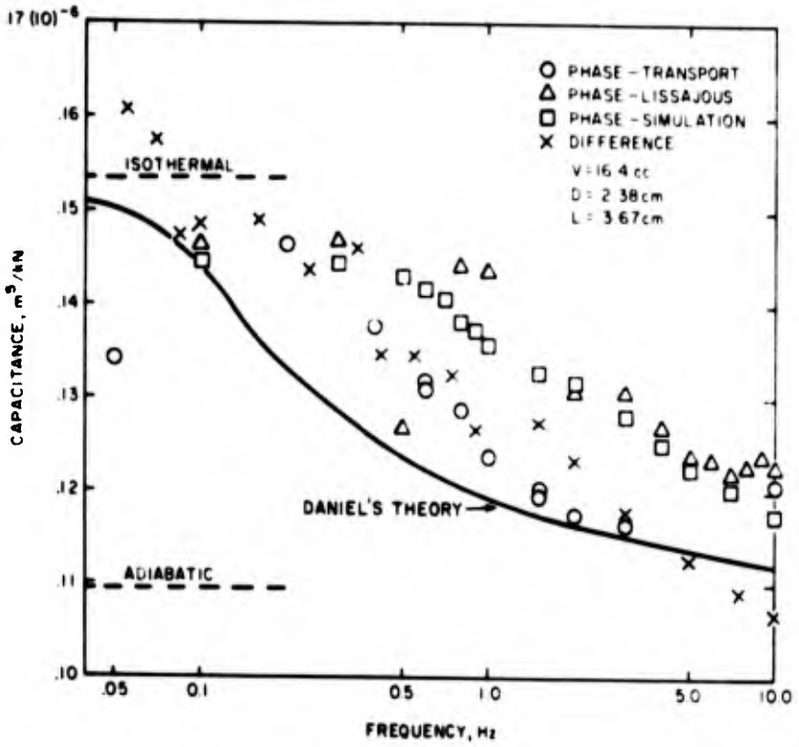

Figure 15. Capacitance vs. Frequency (V = 0.164 (10)$^{-4}$ m^3, D = 2.38 cm.)

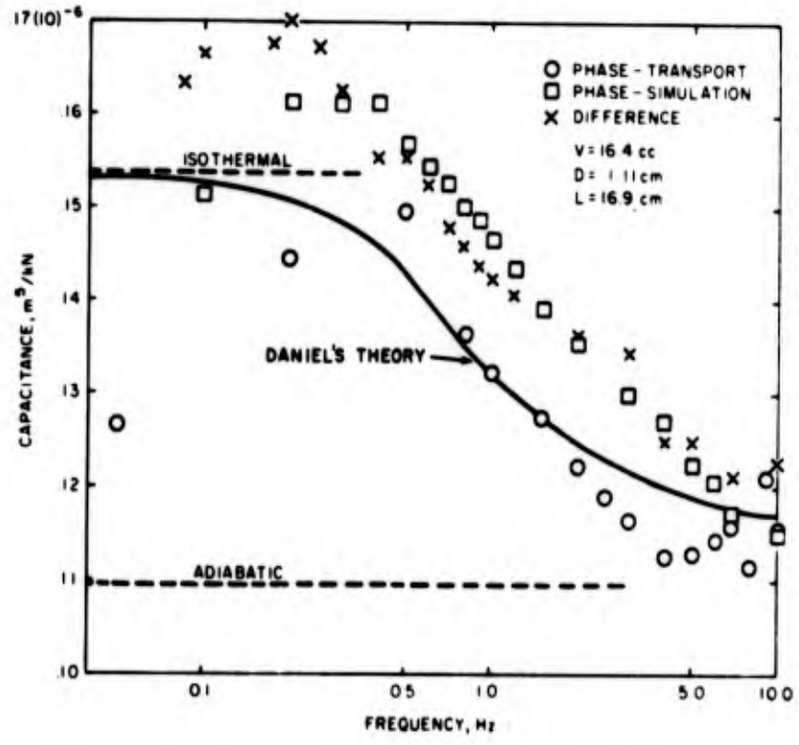

Figure 16. Capacitance vs. Frequency (V = 0.164 (10)$^{-4}$ m^3, D = 1.11 cm)

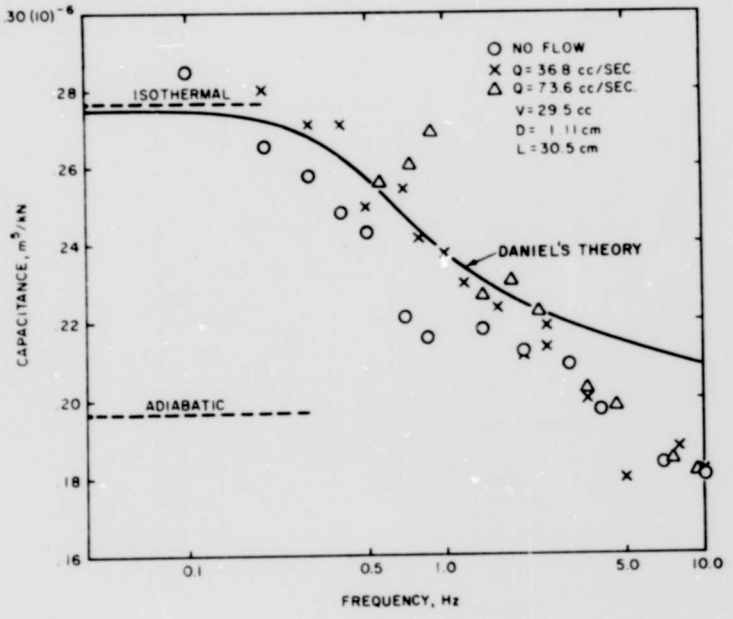

Figure 17. Capacitance vs. Frequency for Tank with Through Flow

Frequency response experiments were performed on fluid RCR circuits to determine whether the transition from isothermal to adiabatic predicted by Daniels' theory is applicable to lumped parameter circuits with moderate signal amplitudes. The capacitance in these experiments were cylindrical tank enclosures. For the diameters and resistors used, the transition occurs at values of ωRC less than 2.0. A sensitivity analysis of the circuit function indicates that phase and difference measurements yield less error augmentation than amplitude measurements. Thus, the capacitance was calculated predominantly from phase and difference measurements.

The experimental results show discrepancies between capacitance calculated from different measuring techniques. Nevertheless the calculated data are always within 20 percent of Daniels' theory for blank chamber tests.

In other experiments with through flow circuits all measurements were taken by the difference method. The results of these tests show that there is only a slight dependency of transition on through flow. The addition of through flow tends to prolong isothermal conditions to higher frequencies. At all flows the data fall within 13 percent of Daniels' theory for zero flow.

We conclude, therefore, that Daniels' theory provides a good indication of poyltropic exponent in lumped parameter fluid circuits at moderate signal levels and with moderate through-flow.

LITERATURE CITED

1. Gibson, J. E. and F. B. Tuteur, "Control System Components," McGraw-Hill Book Company, 1958, p. 447.

2. Zalmanzon, L. A., "Components for Pneumatic Control Instruments," Pergamon Press, 1965, p. 160.

3. Daniels, F. B., "Acoustical Impedance of Enclosures," Journal of the Acoustical Society of America, Volume 19, Number 4, p. 569, July, 1947.

4. Biagi, F. and R. K. Cook, "Acoustic Impedance of a Right Circular Cylindrical Enclosure," Journal of the Acoustical Society of America, Volume 26, Number 4, p. 506, July, 1954.

5. Gerber, H., "Acoustic Properties of Fluid-Filled Chamber at Infrasonic Frequencies in the Absence of Convection," Journal of the Acoustical Society of America, Volume 36, p. 1427, 1964.

6. Gerber, H., "Transient and Sinusoidal Thermal Diffusion, Convection, and Related Infrasonic Pressure Changes in Enclosed, Homogeneous Fluids," U. S. Naval Ordnance Lab., Technical Report 62-94, 1963.

7. Iberall, A. S., "Attenuation of Oscillatory Pressures in Instrument Lines," Journal of Research, National Bureau of Standards, Volume 45, July, 1950, R.P. 2115.

8. Nichols, N. B., "The Linear Properties of Pneumatic Transmission Lines," ISA Transactions, Volume I, No. 1, January, 1962.

9. Brown, F. T., "Pneumatic Pulse Transmission with Bistable-Jet-Relay Reception and Amplification," ScD Thesis, MIT, May, 1962.

10. Schaedel, H., "A Theoretical Investigation of Fluidic Transmission Lines with Rectangular Cross Section," Third Cranfield Fluidics Conference, Paper K3, May, 1968.

11. Kuo, B. C., "Analysis and Synthesis of Sampled-Data Control Systems," Prentice-Hall, 1963.